

# Thermopower of atomic-size metallic contacts

B. Ludoph and J.M. van Ruitenbeek

Kamerlingh Onnes Laboratorium, Universiteit Leiden, Postbus 9504, NL-2300 RA Leiden, The Netherlands

The thermopower and conductance of atomic-size metallic contacts have been simultaneously measured using a mechanically controllable break junction. For contacts approaching atomic dimensions, abrupt steps in the thermopower are observed which coincide with jumps in the conductance. The measured thermopower for a large number of atomic size contacts is randomly distributed around the value for large contacts and can be either positive or negative in sign. However, it is suppressed at the quantum value of the conductance  $G_0 = 2e^2/h$ . We derive an expression that describes these results in terms of quantum interference of electrons backscattered in the banks.

PACS numbers: 72.15.Jf, 72.10.Fk, 73.23.Ad, 73.40.Jn

In recent years stable metallic contacts consisting of a single atom have become experimentally accessible [1]. The interesting interplay between quantization of the electron modes and the atomic structure of the contacts has resulted in intensive research in this field. Information obtained from experiments on atomic-size metallic contacts has mainly been limited to the measurement of the conductance. Two exceptions stand out: the simultaneous measurements of force and conductance by Rubio *et al.* [2], which prove that the conductance steps produced by contact elongation are due to atomic rearrangements, and the measurement of the subgap structure in atomic size superconducting aluminum contacts which characterize the conduction modes, by Scheer *et al.* [3]. In this paper we present measurements of the thermopower in atomic-size metallic contacts.

The thermopower  $S$  is the constant of proportionality between an applied temperature difference  $\Delta\theta$  and the induced voltage,  $V_{tp} = S\Delta\theta$ . The relationship between the thermopower and the electrical conductance  $G$  is given in the linear-response approximation by

$$S = -\frac{\pi^2 k_B^2 \theta}{3e} \frac{\partial \ln G}{\partial \mu},$$

with  $\mu$  the chemical potential. One can view the thermopower as a measure for the difference in conductance between electron and hole quasiparticle excitations, or as the energy dependence of the conductance. We will argue that the dominant contribution to the thermopower in atomic size contacts comes from quantum interference terms as a result of backscattering of electrons on defects near the contact. We have studied the thermopower of atomic-size gold

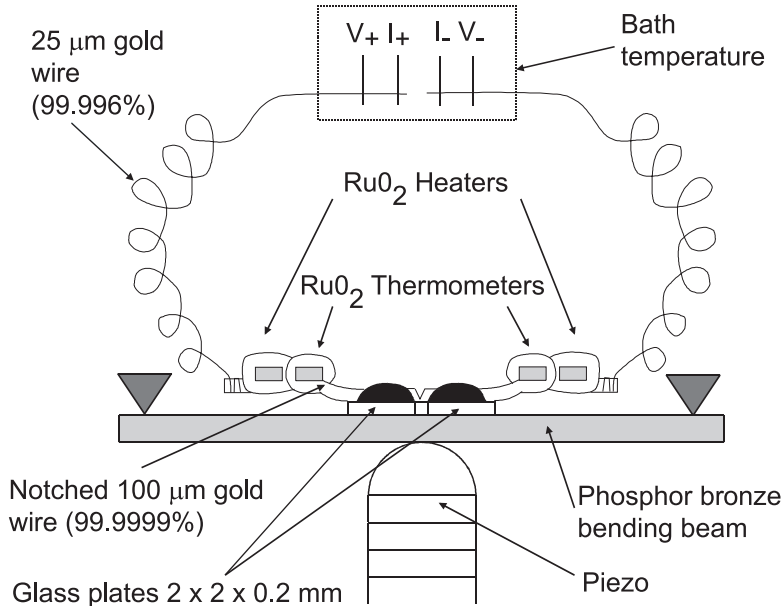


FIG. 1. Schematic diagram of the modified MCB configuration, used for the simultaneous measurement of conductance and thermopower.

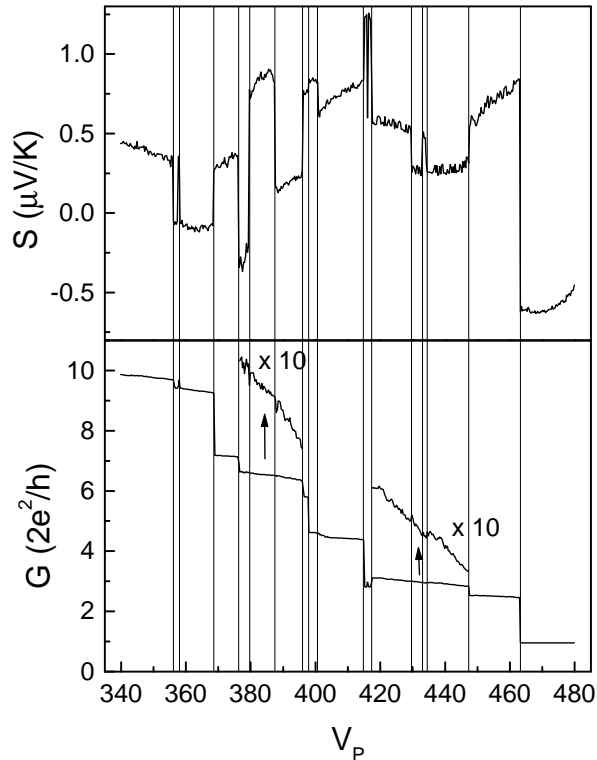


FIG. 2. Typical conductance  $G$  and thermopower  $S$  versus piezovoltage  $V_P$ . The vertical gray lines indicate the corresponding steps in the conductance and thermopower. For two plateaus the conductance scale has been expanded 10 times and offset in order to show the small anomalies in  $G$ .

contacts using a mechanically controllable break junction (MCB) [4]. A schematic diagram of the sample configuration is shown in Fig. 1. By bending the phosphor bronze substrate, the  $100\ \mu\text{m}$  gold wire breaks at the notch, allowing atomic-size contacts to be adjusted. This gold wire is attached to long thin ( $25\ \mu\text{m}$ ) gold wires at both ends. They connect the notched wire to the current and voltage leads, anchored at the bath temperature, hence forming an open gold loop. The central gold wire is tightly wound and varnished on each side of the contact around a calibrated  $5\ \text{k}\Omega$   $\text{RuO}_2$  thermometer and a  $500\ \Omega$   $\text{RuO}_2$  heater. Using one heater, a temperature gradient over the contact can be applied. The glass plates and thin gold wires serve as thermal resistances to the substrate and bath temperatures, respectively. The sample is placed in a regular MCB setup in an evacuated can immersed in liquid helium. The conductance and thermopower were measured in three steps: The voltage over the contact was measured with a nanovoltmeter at  $-100\ \text{nA}$ ,  $+100\ \text{nA}$  and at zero dc current bias, while maintaining a constant temperature gradient over the contact by applying about  $2\ \text{mW}$  heating power to a heater on one side of the constriction. The conductance is then obtained from the voltage difference for the two current polarities, and  $S$  is obtained from the voltage at zero bias current. Each cycle takes about  $4\ \text{s}$  and is continuously repeated as we slowly sweep the piezovoltage up in order to decrease the contact size. A curve (Fig. 2) was generally taken from  $10G_0$  to tunneling in  $30\ \text{min}$  ( $G_0$  is the quantum conductance unit,  $2e^2/h$ ). Every few traces, it was necessary to readjust the contact manually, which inevitably leads to the contact being pushed completely together. Low pass RC filters ( $10\ \text{Hz}$ ) were mounted in the circuit near the sample to prevent rectification of ac disturbances by the asymmetry of the voltage dependence of the conductance. Extensive measurements have been performed on two samples (referred to as samples 1 and 2).

The primary limitation of the sample design is the thickness of the glass plates and thus the thermal insulation of the gold sample wire from the phosphor bronze substrate. The thickness is a trade-off between stability and thermal insulation. As a result of thermal currents flowing to the substrate, a thermal gradient is established in the sample wire between the thermometer and the contact. The measured temperature is hence not the actual temperature of the “hot” side of the constriction. We calibrate this thermal gradient by measuring the thermopower for large contacts, with resistances in the range  $1 - 10\ \Omega$ , as a function of heating power. First, we stress that the thermal resistance of the contact is orders of magnitude larger than that of the wire on either side, therefore the temperature difference over the contact can be taken to be independent of the contact size. This is corroborated by experiment, which shows that the mean value of the thermopower over the contact as a function of contact diameter in the range  $0.1 - 100\ \Omega$

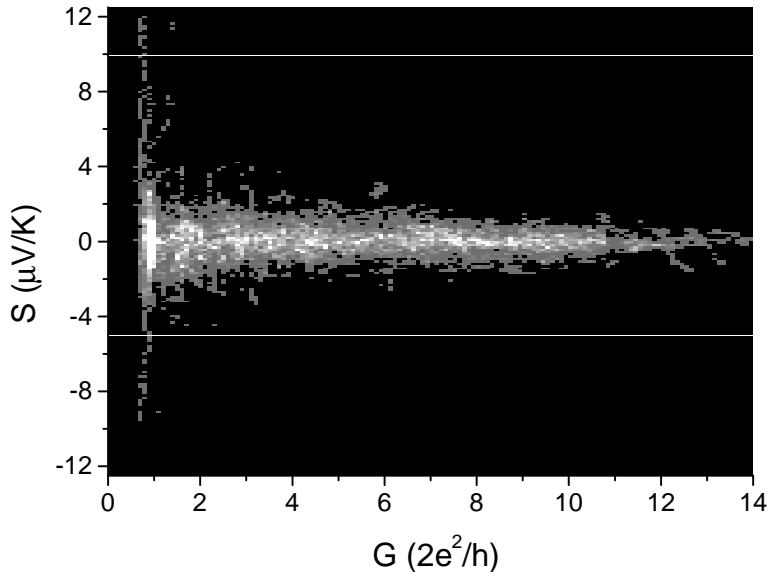


FIG. 3. Density plot of thermopower against conductance: The thermopower axis is divided into  $0.125 \mu\text{V}/\text{K}$ , and the conductance into  $0.1G_0$  sections, creating  $0.125 \mu\text{V}/\text{K}$  by  $0.1G_0$  bins. The occurrence of a particular combination of conductance and  $S$  is added to its corresponding bin, and the sum of 220 curves for the two samples is plotted in gray scale above. Black represents no data points and white more than 100. We note that above  $10 G_0$  fewer data have been taken.

remains constant within an accuracy of 1%. We take advantage of the fact that for conventional point contacts the phonon drag contribution to the thermopower becomes negligible [5]. Since the contact is part of a uniform gold loop, the measured thermopower corresponds to the phonon drag contribution of the leads only. The side that is not heated remains equal to the substrate temperature and we assume that the actual temperature difference over the contact is a fixed fraction,  $\alpha$ , of the measured temperature difference. We then determine this fraction by comparing the measured large-contact thermopower as a function of temperature with literature values for the bulk thermopower of pure gold [6,7], which is nearly linear between 10 and 25 K, with a slope of  $\sim 0.05 \mu\text{V}/\text{K}^2$ . For the two gold samples discussed below, the model provides a good description when the fraction  $\alpha$  is taken as 0.4 and 0.5, respectively. We estimate an error of about 20% for the temperature difference obtained.

To have a reasonable signal level we need to apply a temperature difference of several kelvins. In the case of sample 1 the temperature difference  $\Delta\theta = 4 \text{ K}$ , and the average of the temperatures on both sides of the contact is  $\theta_{av} = 11.5 \text{ K}$ . For sample 2,  $\Delta\theta = 6 \text{ K}$  and  $\theta_{av} = 12 \text{ K}$ . As it is not obvious that this  $\Delta\theta$  can be regarded as a small (linear) perturbation, we will take the full dependence of  $S$  on  $\Delta\theta$  into account in the analysis below. For all the results presented below, the bulk thermopower of the leads has been subtracted.

While breaking the contact by increasing the piezovoltage, the usual plateaus in the conductance are observed [1,2,4,8]. When heating one side of the contact we observe steps in the thermopower which occur simultaneously with conductance jumps from one plateau to the next. Each measured curve produces a different conductance and thermopower trace and a typical example is shown in Fig. 2. Even tiny jumps or changes of slope of the conductance can be accompanied by large steps in the thermopower. On a conductance plateau, even though the conductance hardly changes, smooth variations in the thermopower are usually observed. Note that the thermopower of the contact can have both a positive or negative sign. When we do not heat, or heat both sides of the contact to the same temperature, we observe no thermopower voltage within the noise level of 300 nV peak to peak.

In order to obtain statistical information about a possible correlation between the measured thermopower and conductance values, a density plot was constructed from the combined data of the 72 and 148 individual curves from sample 1 and 2, respectively (Fig. 3). The conductance axis was divided into 10 partitions per  $G_0$  and the thermopower axis in partitions of  $0.125 \mu\text{V}/\text{K}$ . Then, the number of data points falling in each range of conductance and thermopower was counted and the results are represented in gray scale in Fig. 3. In this figure we observe an increase in the spread of the thermopower values with decreasing contact size, with both positive and negative sign.

A conductance histogram of the 220 curves is, within the statistical accuracy, in agreement with other gold histograms taken at low temperatures (e.g. Ref. [9]). Although the data are not presented here, similar results for the thermopower have also been observed in silver and copper samples, albeit for a more limited number of curves.

The thermopower has a random value and sign, and seems to be much more sensitive to small changes in the

atomic geometry of the contact than the conductance. This is not expected from the simple adiabatic models for point contacts, which only predict a positive sign [10,11]. We propose an interpretation of this behavior in terms of coherent backscattering of the electrons near the contact: As a result of the interference of waves with different path length, the transmission of the contact will show fluctuations as a function of energy [12,13]. Each atomic rearrangement at a conductance step will alter the interference paths of the backscattered electrons by a significant fraction of  $\lambda_F$ , and hence change the energy dependence of the transmission in an unpredictable way causing each step in the conductance to result in an unpredictable jump in the thermopower. Along a plateau, the contact gradually changes position with respect to the scattering centers nearby and a gradual change in the interference pattern occurs.

We now derive an expression for the thermopower based on these concepts. The thermopower in quantum point contacts can be written as  $S = -L/G$ , with [10,11]:

$$\frac{L}{G} = \frac{\frac{2e}{h} \int_0^\infty (\text{Tr } \mathbf{t} \mathbf{t}^\dagger) [f(\theta + \Delta\theta, E) - f(\theta, E)] dE}{\frac{2e^2}{h} \int_0^\infty (\text{Tr } \mathbf{t} \mathbf{t}^\dagger) \frac{\partial f}{\partial E} dE},$$

where  $(\text{Tr } \mathbf{t} \mathbf{t}^\dagger)$  is the sum of the transmission probabilities,  $f(\theta, E)$  is the temperature- and energy-dependent Fermi function,  $h$  is Planck's constant, and  $e = |e|$  is the electron charge. The thermopower is characterized by the energy dependence of the transmission probabilities. We have approached the problem using the same method as presented in Ref. [14] for the derivation of the conductance fluctuations in atomic size contacts. The point contact is taken as a ballistic central constriction with diffusive regions on both sides. The ballistic section (using the Landauer-Büttiker formalism) is characterized by  $N$  conductance modes, each with a transmission probability  $T_n$  and a contribution  $T_n G_0$  to the conductance. After transmission through the contact, within the dephasing time  $\tau_\phi$ , the electron scatters elastically in the diffusive region and has a finite probability amplitude,  $a$ , to return to the contact. When the diameter of the contact is small compared to the elastic scattering length  $l_e$ , the return probability,  $|a|^2$ , is small and we need only consider lowest-order processes. To lowest order in  $a$  we can write the transmission of the three sections combined as

$$\text{Tr } \mathbf{t} \mathbf{t}^\dagger = \sum T_n [1 + 2\text{Re} (r_n a_{l,n} + r'_n a_{r,n})]. \quad (1)$$

Here,  $r_n$  and  $r'_n$  are the reflection coefficients in the transfer matrix describing the central ballistic section of the contact when coming from the left and right, respectively, with  $|r_n|^2 = |r'_n|^2 = 1 - T_n$ .  $a_{l,n}$  and  $a_{r,n}$  are the return amplitudes for mode  $n$  from the left and right diffusive regions, respectively. The latter are sums over all possible paths of length  $l$ , containing phase factors  $e^{i(E-E_F)l/v_F\hbar}$ . The second term in Eq. (1) describes the interference of the directly transmitted wave with the fraction that, after transmission, is first backscattered to the contact and subsequently *reflected* at the contact. Assuming the dominant energy dependence is in the phase factors, the integration over  $E$  in the expression for  $L$  can be performed. We consider the square of  $L$ , averaged over an ensemble of scattering configurations,

$$\langle L^2 \rangle = \left( \frac{2ek_B}{h} \frac{\theta}{\Delta\theta} \right)^2 \sum_n T_n^2 (1 - T_n) \int_0^\infty \langle |a(\tau)|^2 \rangle \left( \frac{1}{\sinh(z)} - \frac{1 + \Delta\theta/\theta}{\sinh(z(1 + \Delta\theta/\theta))} \right)^2 d\tau, \quad (2)$$

with  $z = \pi k_B \theta \tau / \hbar$  and  $\tau = l/v_F$ . Here we have assumed that  $a_{l,n}$  and  $a_{r,n}$  are uncorrelated and have the same average return probability  $\langle |a|^2 \rangle$ , independent of the mode number  $n$ .

For  $\langle |a(\tau)|^2 \rangle$  we substitute the semiclassical probability to return to the contact into any of the  $N$  modes after a time  $\tau$ ,  $\langle |a(\tau)|^2 \rangle = v_F / [\sqrt{12\pi} k_F^2 (D\tau)^{3/2}]$ , with  $D = v_F l_e / 3$  the diffusion constant. The integral in Eq. (2) can be performed numerically. It only weakly depends on the ratio  $\Delta\theta/\theta$ . For the standard deviation of the thermopower  $\sigma_S = \sqrt{\langle S^2 \rangle - \langle S \rangle^2} = \sqrt{\langle L^2 \rangle / \langle G^2 \rangle}$  this finally results in

$$\sigma_S = \frac{ck_B}{e k_F l_e \sqrt{1 - \cos \gamma}} \left( \frac{k_B \theta}{\hbar v_F / l_e} \right)^{1/4} \frac{\sqrt{\sum_{n=1}^N T_n^2 (1 - T_n)}}{\sum_{n=1}^N T_n}. \quad (3)$$

Here,  $c$  is a numerical constant which equals 5.658 in the limit  $\Delta\theta/\theta \rightarrow 0$ , and increases by about 5% for  $\Delta\theta/\theta = 0.5$ . We have also introduced a factor  $(1 - \cos \gamma)$  to account for the finite geometrical opening angle of the contact, where the limit  $\gamma = 90^\circ$  corresponds to an opening in an infinitely thin insulating layer between two metallic half spaces. Note that  $\sigma_S$  in Eq. (3) is equal to zero when all  $T_n$  are equal to either 0 or 1.

In Fig. 4 we plot the standard deviation of the thermopower, determined from the experimental data by sorting all data points as a function of  $G$  from the combined set of the 220 curves and averaging over 1000 consecutive data points. We compare these data to the theoretical curve calculated from the above expression for the case where the

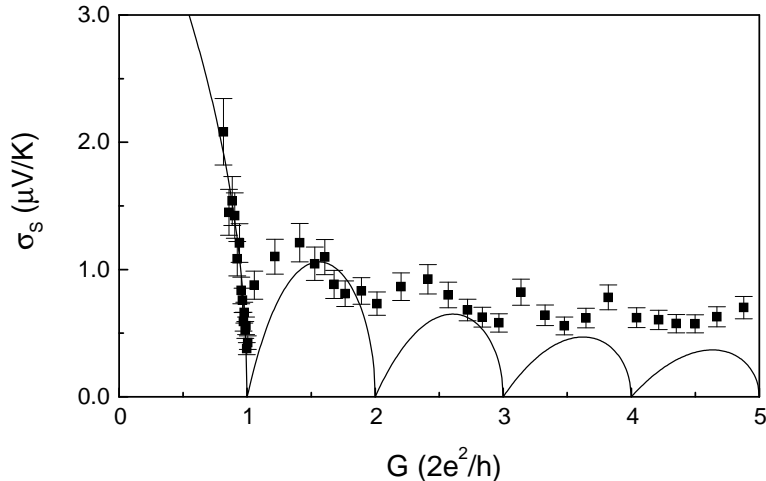


FIG. 4. Standard deviation of the thermopower against conductance. Solid squares represent the measured data and the solid line is the theoretical curve assuming the conductance modes open one by one.

modes contributing to the conductance open one by one. That is, for all conductances with  $N$  modes contributing to the conductance, only one (i.e.,  $T_N$ ) differs from 1 and  $\sigma_S \propto T_N \sqrt{1 - T_N} / (N - 1 + T_N)$ . The observed deep minimum at  $G = G_0$  suggests that this conductance is dominantly carried by a single mode. This is in agreement with measurements of the shot noise on atomic size gold contacts [15], and the observed suppression of conductance fluctuations in Ref. [14]. For  $G > G_0$ , the limited statistics in combination with the property that the effect in the thermopower scales inversely with conductance prevent the definite identification of minima near quantized values.

From the amplitude of the curve we obtain an estimate for the elastic mean free path of  $l_e = 5 \pm 1$  nm, using reasonable values for the opening angle of the contact of  $35^\circ$ – $50^\circ$  [16]. All data points should be on or above the full curve in Fig. 4, since contributions by more conductance modes can only increase the variance in the thermopower. Therefore,  $l_e$  cannot be much smaller than 4 nm. For a much larger value of  $l_e$  many modes would have to contribute to the conductance, in which case we would not expect to find any minima at quantized values.

Apart from the thermopower effects described here, for a quantum point contact positive peaks in the thermopower, centered at conductance values  $(n + \frac{1}{2})G_0$ ,  $n = 0, 1, 2, \dots$ , were predicted due to the structure of the electron density of states [10,11]. This effect has indeed been observed in two-dimensional electron gas devices [17], but is much smaller than the fluctuations we observe here, and therefore cannot be resolved in the mean value  $\langle S \rangle$  for our metallic point contacts.

The mechanism we present to explain the thermopower is the same as the one proposed for the voltage dependence of the conductance [14]. Indeed, when we plot  $\sigma_S$  and  $\sqrt{\langle (\partial G / \partial V)^2 \rangle} / G$  for gold, the data show very similar behavior. The energy scales with which both measurements have been performed are so different (6 K temperature difference versus 20 mV amplitude) that comparison between the parameters obtained by both methods is a test for the validity of the theoretical derivation. The mean free path value obtained from the conductance fluctuations is 5 nm, in good agreement with the estimate obtained here. Hence, the fact that both works are not only in good qualitative but also in good quantitative agreement is strong support for the model used.

This work was part of the research program of the “Stichting FOM”, which was financially supported by NWO. We have greatly profited from many discussions with C. Urbina, D. Esteve, M.H. Devoret, and we thank L.J. de Jongh for his stimulating support.

- 
- [1] J.K. Gimzewski and R. Möller, Phys. Rev. B **36**, 1284 (1987); J.M. Krasns *et al.*, Phys. Rev. B **48**, 14721 (1993).
  - [2] G. Rubio, N. Agraït and S. Vieira, Phys. Rev. Lett. **76**, 2302 (1996).
  - [3] E. Scheer *et al.*, Phys. Rev. Lett. **78**, 3535 (1997).
  - [4] C.J. Muller, J.M. van Ruitenbeek and L.J. de Jongh, Physica C **191**, 485 (1992).

- [5] O.I. Shklyarevskii *et al.*, Phys. Rev. Lett. **57**, 1374 (1986).
- [6] W.B. Pearson, Sov. Phys. Solid State **3**, 1024 (1961).
- [7] A.M. Guénault and D.G. Hawksworth, J. Phys. F **7**, L219 (1977).
- [8] J.I. Pascual *et al.*, Phys. Rev. Lett **71**, 1852 (1993).
- [9] C. Sirvent *et al.*, Physica B **218**, 238 (1996).
- [10] P. Strada, J. Phys. Condens Matter **1**, 1025 (1989); H. van Houten *et al.*, Semicond. Sci. Technol. **7**, B215 (1992).
- [11] E.N. Bogachek, A.G. Scherbakov and U. Landman, Phys. Rev. B **54**, R11 094 (1996).
- [12] A.I. Larkin and D.E Khmel'nitskii, Zh. Eksp. Teor. Fiz. **91**, 1815 (1986) [Sov. Phys. JETP **64** 1075 (1986)]; Yu. V. Nazarov, *ibid.* **98**, 306 (1990) [**71**, 171 (1990)]; A. Yu. Zyuzin and B.Z. Spivak, *ibid.* **98**, 1011 (1990) [**71**, 563 (1990)]; D.L. Maslov, C. Barnes and G. Kirczenow, Phys. Rev. Lett. **70**, 1984 (1993).
- [13] This interference is also responsible for fluctuations in the conductance observed for much larger contacts: P.A.M. Holweg *et al.*, Phys. Rev. Lett. **67**, 2549 (1991); P.A.M Holweg *et al.*, Phys. Rev. B **48**, 2479 (1993); D.C. Ralph, K.S. Ralls and R.A. Buhrman, Phys. Rev. Lett. **70**, 986 (1993).
- [14] B. Ludoph *et al.*, cond-mat/9810384; Phys. Rev. Lett. **82**, 1530 (1999).
- [15] H.E. van den Brom and J.M. van Ruitenbeek, cond-mat/9810276; Phys. Rev. Lett., **82**, 1526 (1999).
- [16] C. Untiedt *et al.*, Phys. Rev B **56**, 2154 (1997).
- [17] L.W. Molenkamp *et al.*, Phys. Rev. Lett. **65**, 1052 (1990).